γ_0 = zero shear normal stress coefficient, dynes-sec.^{2}/sq.cm.
$\eta(K)$ = viscosity function, Equation (8), dynes-sec./sq.cm.
η_0 = zero shear viscosity, dynes-sec./sq.cm.
τ_{ij} = stress tensor
$\tau_{rr}, \tau_{\theta\theta}$ = r and θ components of stress, dynes/sq.cm.
θ = polar coordinate

LITERATURE CITED

1. Adams, E. B., Ph.D. dissertation, Univ. Tennessee, Knoxville (Aug., 1967).
2. ———, J. C. Whitehead, and D. C. Bogue, *AIChE J.*, **11**, 1026 (1965).
3. Bernstein, B., E. A. Kearsley, and L. J. Zapas, *Trans. Soc. Rheo.*, **7**, 391 (1963); **9**, 27 (1965).
4. ———, *J. Res. Natl. Bur. Stds.*, **68B**, 103 (1964).
5. Bogue, D. C., and J. O. Doughty, *Ind. Eng. Chem. Fundamentals*, **5**, 243 (1966).
6. Doughty, J. O., Ph.D. dissertation, Univ. Tennessee, Knoxville (July, 1966).
7. ———, and D. C. Bogue, *Ind. Eng Chem. Fundamentals.*, **6**, 388 (1967).
8. Ferry, J. D., "Viscoelastic Properties of Polymers," John Wiley, New York (1960).
9. Fields, T. R., Jr. ,and D. C. Bogue, *Trans. Soc. Rheol.*, **12:1**, 39 (1968).
10. Metzner, A. B., J. L. White, and M. M. Denn, *AIChE J.*, **12**, 863 (1966).
11. Spriggs, T. W., J. D. Huppler, and R. B. Bird, *Trans. Soc. Rheol.*, **10**, 191 (1966).
12. Tobolsky, A. V., "Properties and Structure of Polymers," John Wiley, New York (1960).
13. White, J. L., and N. Tokita, *J. Phys. Soc., Japan*, **22**, 719 (1967).
14. Zapas, L. J., *J. Res. Natl. Bur. Stds.*, **70A**, 525 (1966).
15. ———, and T. Craft, *ibid.*, **69A**, 541 (1965).

Manuscript received February 15, 1968; revision received July 15, 1968; paper accepted July 18, 1968.

Numerical Evaluation of Temperature Profiles and Interface Position in Filaments Undergoing Solidification

MILTON E. MORRISON

Aerospace Research Laboratories, Wright-Patterson Air Force Base, Ohio

A numerical method has been described for the solution of the general equations which depict solidification in the cylindrical coordinate system. The method has been outlined for cooling and solidification of a moving filament of molten polymer. The solution is given in terms of six dimensionless variables: α_l/α_s, k_l/k_s, hR/k_R, $L/[C_{ps}(T_o-T_c)]$, T_o/T_c, and $\sigma\epsilon_p R(T_o-T_c)^3/k_R$. Plots are shown for the solution of the heat transfer equations and associated boundary conditions for several values of the dimensionless variables. The method describes the process of cooling and freezing liquids when convective and/or radiative energy losses are considered. The form of the theoretical equation compares very favorably with experimental data.

Prediction of the temperature profile and solid-liquid interface as a function of time for a freezing medium is of importance in the processing of frozen foods, casting of metals and solid rocket motors, production of plastic components, and spinning of textile fibers. It is important to know the position of the solid-liquid interface as a function of time in order to determine the time for solidification. However, in some instances it is even more important to know the temperature profile as a function of time. In the spinning of many textile fibers, molten polymer is extruded through an orifice and the filament cooled by passing through an inert gaseous atmosphere. The fiber properties are then altered by a drawing process. If the fiber is not sufficiently cooled or large temperature gradients exist during the spinning process, filaments with undesirable properties may result. This paper describes the numerical solution of a set of partial differential equations which describe heat transfer in a freezing filament. Radial temperature profiles and interface position are evaluated as a function of time. The filament is initially liquid and above the freezing point; however, simpler problems such as heat transfer to a saturated solution can also be solved by the technique described.

Several papers have been published on heat transfer in freezing media. London and Seban (*17*) presented an analogue method for prediction of the solid-liquid interface position as a function of time when the specific heat of the two phases was neglected. Their work considered the freezing problem in cartesian, cylindrical, and spherical coordinate systems. Danckwerts (*8*) obtained solutions for heat conduction with a moving boundary in cartesian coordinates, when the change in density was important. Lin (*16*) has presented an analytical solution for the liquid-solid interface position as a function of time for unsteady state freezing problems in the cylindrical and spherical coordinate system, if the cartesian coordinate solution is known. Relaxation methods were used to solve the cartesian coordinate problem in a semi-infinite medium by Allen and Severn (*1*). Hrycak (*11*) has described solidification of a plane-parallel stratified medium. Carslaw and Jaeger (*5*) report a solution for freezing a saturated liquid in a semi-infinite medium in cartesian coordinates. Wilcox and Duty (*22*) have described a numerical technique for evaluation of steady state temperature profiles in a cylindrical crystal being drawn from a liquid melt. Numerical methods for solution of the unsteady state freezing problem

Milton E. Morrison is with American Enka Corporation, Enka, North Carolina.

have been reported by Tao (*21*) and Crank (*7*). Crank considered the cartesian coordinate system, while Tao reported results for freezing of a saturated liquid in cylinders and spheres. Longwell (*18*) reported a graphical method for solution of the freezing problem which was applicable to a cartesian, cylindrical, or spherical coordinate system.

NUMERICAL METHOD AND RESULTS

Consider a filament of liquid polymer extruded through an orifice at a temperature T_0 into an inert atmosphere at T_c as shown in Figure 1. The liquid can be extruded at the freezing point T_f or at some higher temperature. By consideration of an energy balance (3) in one phase of the filament at a distance (z) from the orifice, the following equation results:

$$\rho C_p \frac{DT}{Dt} = \nabla \cdot k\nabla T + \left(\frac{\partial \ln V}{\partial \ln T}\right)_p \frac{DP}{Dt} - \gamma_v : \nabla v \quad (1)$$

For the given problem, Equation (1) can be simplified considerably by assuming steady state conditions, no viscous dissipation, constant filament velocity, constant thermal diffusivity, no pressure gradients, symmetry about the filament axis, negligible longitudinal conduction, and no radial velocity component. Using these assumptions for the liquid phase, Equation (1) reduces to:

$$v_z \frac{\partial T_l}{\partial z} = \frac{\alpha_l}{r} \frac{\partial}{\partial r}\left(r \frac{\partial T_l}{\partial r}\right) \quad (2)$$

For the solid phase

$$v_z \frac{\partial T_s}{\partial z} = \frac{\alpha_s}{r} \frac{\partial}{\partial r}\left(r \frac{\partial T_s}{\partial r}\right) \quad (3)$$

At the solid-liquid interface the temperature is continuous, therefore Equation (4)

$$@\ r = r^* \quad T_s = T_l = T_f \quad (4)$$

requires that the energy liberated by freezing be transferred from the solid-liquid interface or

$$-k_l \frac{\partial T_l}{\partial r}\bigg|_{r^*} + k_s \frac{\partial T_s}{\partial r}\bigg|_{r^*} - L\rho_s \frac{dr^*}{d\left(\frac{z}{v_z}\right)} = 0 \quad (5)$$

The system is completely described by Equations (2) through (5) and the associated initial and boundary conditions:

initial condition: $@\ z = 0,\ T = T_0$

boundary condition 1: $@\ r = 0,\ \dfrac{\partial T}{\partial r} = 0$

boundary condition 2: $@\ r = R,\ q_R = -k_R \dfrac{\partial T}{\partial r}\bigg|_R = h(T_R - T_c)$ (6)

boundary condition 3: $@\ r = r^*,\ T = T_f$

The problem can be somewhat simplified by consideration of four dimensionless variables

$$\gamma = \frac{T - T_c}{T_0 - T_c} \quad (7)$$

$$\xi = \frac{r}{R} \quad (8)$$

$$\Omega = \frac{z\alpha}{v_z R^2} \quad (9)$$

$$\zeta = \frac{L}{C_{ps}(T_0 - T_c)} \quad (10)$$

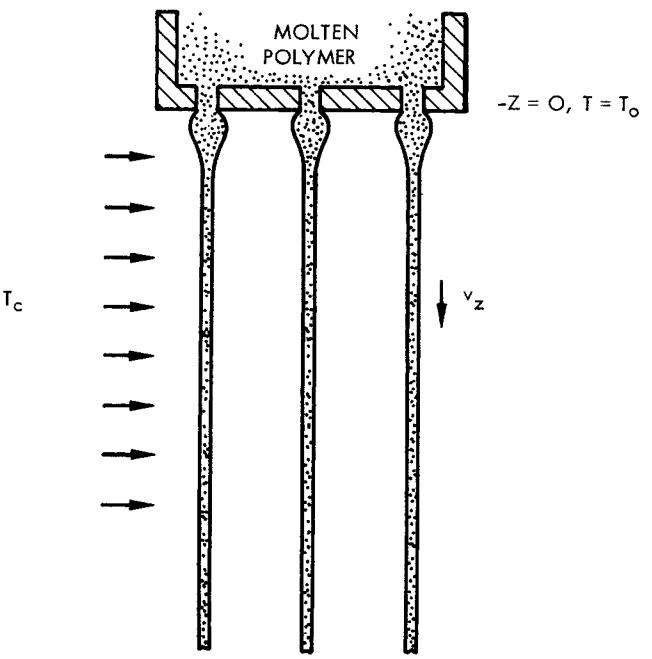

Fig. 1. Schematic of fiber spinning technique.

Incorporation of the dimensionless variables into Equations (2) through (6) yields the final mathematical formulation.

$$\frac{\partial \gamma_l}{\partial \Omega_l} = \frac{1}{\xi} \frac{\partial}{\partial \xi}\left(\xi \frac{\partial \gamma_l}{\partial \xi}\right) \quad (11)$$

$$\frac{\partial \gamma_s}{\partial \Omega_s} = \frac{1}{\xi} \frac{\partial}{\partial \xi}\left(\xi \frac{\partial \gamma_s}{\partial \xi}\right) \quad (12)$$

$$\frac{d\xi^*}{d\Omega_s} = \frac{1}{\zeta} \frac{\partial \gamma_s}{\partial \xi}\bigg|_{\xi^*} - \frac{k_l}{\zeta k_s} \frac{\partial \gamma_l}{\partial \xi}\bigg|_{\xi^*} \quad (13)$$

initial condition: $@\ \Omega = 0,\ \gamma = 1$

boundary condition 1: $@\ \xi = 0,\ \dfrac{\partial \gamma}{\partial \xi} = 0$

boundary condition 2: $@\ \xi = 1,\ \dfrac{\partial \gamma}{\partial \xi}\bigg|_R = -\gamma_R\left(\dfrac{hR}{k_R}\right)$ (14)

boundary condition 3: $@\ \xi = \xi^*,\ \gamma = \gamma_f$

Solution of the problem involves cooling the liquid polymer until the surface of the filament reaches the freezing point. That requires only Equations (11) and (14). Then the filament begins to freeze. During the freezing process Equations (11) through (14) must be solved simultaneously. After the filament is completely solidified, the cooling of the solid strand to the temperature of the surroundings, T_c, is continued. The cooling of the liquid filament, which means solution of Equation (11) with the initial and boundary conditions results in the following equation (*6*):

$$\gamma = 2 \sum_{n=1}^{\infty} \frac{\alpha_n J_1(\alpha_n)\, J_0(\alpha_n \xi)\, e^{-\alpha_n^2 \Omega}}{\left[\left(\dfrac{hR}{k_R}\right)^2 + \alpha_n^2\right] J_0^2(\alpha_n)} \quad (15)$$

where α_n is the root of

$$\alpha_n J_1(\alpha_n) = \frac{hR}{k_R} J_0(\alpha_n) \quad (16)$$

Although an analytical solution can be obtained for the cooling problem, a numerical method must be used to describe the freezing of liquid polymer as described by Equations (11) through (14). That numerical problem

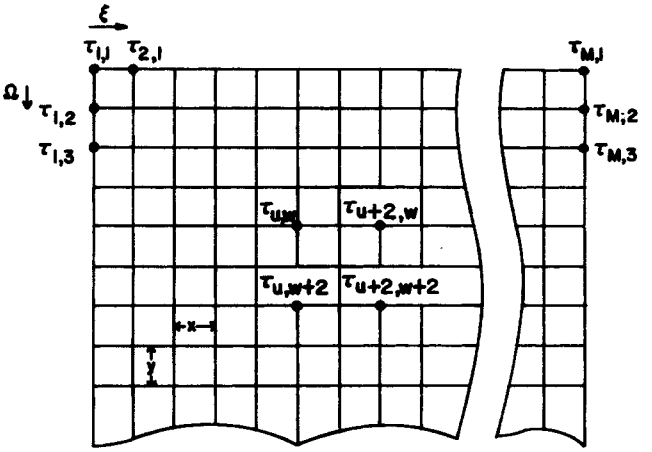

Fig. 2. Rectangular grid for representation of numerical solution.

requires simultaneous solution of parabolic partial differential equations. An implicit form of difference equation for the differentials was used, since convergence requirements are not as restricted for implicit as for the explicit forms (*20*). The following difference equations were used in this work.

$$\frac{\partial^2\gamma}{\partial\xi^2} = \frac{1}{2x^2}\left[\gamma_{u+1,\,w+1} - 2\,\gamma_{u,\,w+1} + \gamma_{u-1,\,w+1}\right)$$

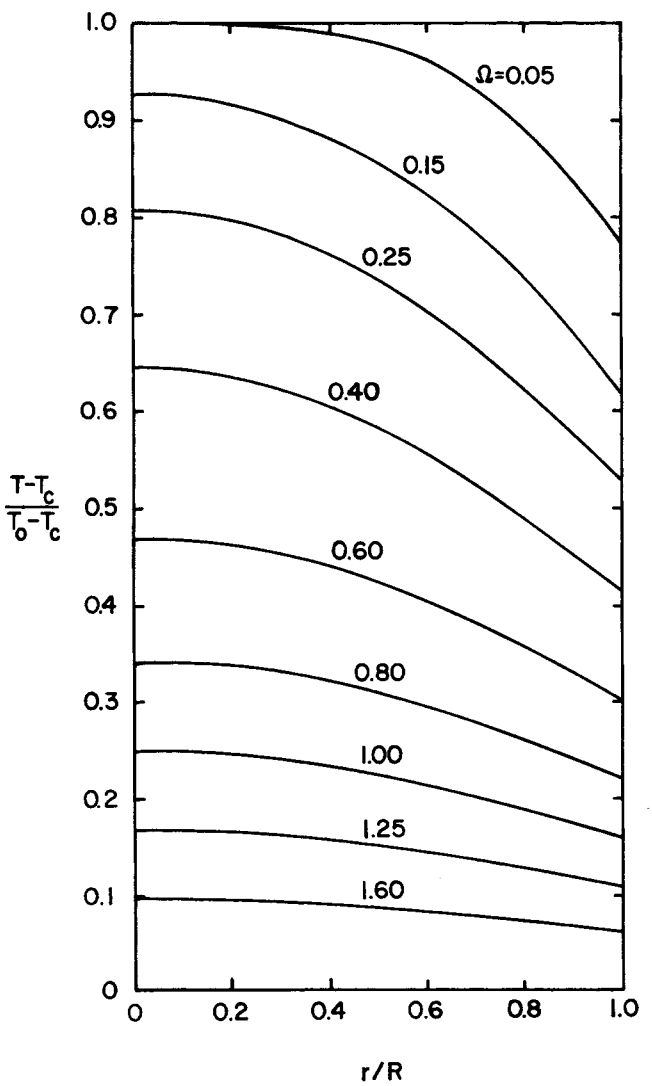

Fig. 3. Dimensionless temperature vs. radius for $hR/k_R = 1$, when $k_l/k_s = 1$, $\alpha_l/\alpha_s = 1$, $\beta = 0$, and $L/[C_{ps}(T_o - T_c)] = 0$.

$$+ \left(\gamma_{u+1,\,w} - 2\,\gamma_{u,\,w} + \gamma_{u-1,\,w}\right)] \quad (17)$$

$$\frac{\partial\gamma}{\partial\xi} = \frac{1}{4x}\left[\gamma_{u+1,\,w+1} - \gamma_{u-1,\,w+1}) + (\gamma_{u+1,\,w} - \gamma_{u-1,\,w})\right] \quad (18)$$

$$\frac{\partial\gamma}{\partial\Omega} = \frac{\gamma_{u,\,w+1} - \gamma_{u,\,w}}{y} \quad (19)$$

Each point in the difference grid is represented as u in the ξ direction and w in the Ω direction where x is the distance betweeen successive u points and y is the distance between successive w points. The difference grid is shown schematically in Figure 2.

After using the difference representations given in Equations (17) through (19), Equations (11) through (14) reduce to

$$A_u\gamma_{u+1,\,w+1} + B_u\gamma_{u,\,w+1} + C_u\gamma_{u-1,\,w+1} = D_u \quad (11a) \text{ or } (12a)$$

where

$$A_u = \frac{1}{2x^2} + \frac{1}{4x\xi}$$

$$B_u = -\frac{1}{x^2} - \frac{1}{y}$$

$$C_u = \frac{1}{2x^2} - \frac{1}{4x\xi}$$

$$D_u = -\gamma_{u+1,\,w}\left(\frac{1}{2x^2} + \frac{1}{4x\xi}\right) - \gamma_{u,\,w}\left(\frac{1}{y} - \frac{1}{x^2}\right) - \gamma_{u-1,\,w}\left(\frac{1}{2x^2} - \frac{1}{4x\xi}\right)$$

$$\frac{\xi^*_{w+1} - \xi^*_w}{y_s} = \frac{1}{2x\zeta}\left(\gamma_{f+1,\,w+1} - \gamma_{f,\,w+1} + \gamma_{f+1,w} - \gamma_{f,\,w}\right) - \frac{k_l}{2\zeta k_s x}\left(\gamma_{f,\,w+1} - \gamma_{f-1,\,w+1} + \gamma_{f,\,w} - \gamma_{f-1,\,w}\right) \quad (13a)$$

initial condition: @ $\Omega = 0$, $\gamma_{u,\,1} = 1$

boundary condition 1: @ $\xi = 0$

$$\frac{2}{x^2}\gamma_{2,\,w+1} + B_1'\,\gamma_{1,\,w+1} = D_1'$$

$$B_1 = -\frac{2}{x^2} - \frac{1}{k}$$

$$D_1 = -\frac{2}{x^2}\gamma_{2,\,w} - \gamma_{1,\,w}\left(\frac{1}{y} - \frac{2}{x^2}\right) \quad (14a)$$

boundary condition 2: @ $\xi = 1$

$$B_M'\,\gamma_{M,\,w+1} + \frac{1}{x^2}\gamma_{M-1,\,w+1} = D_M'$$

$$B_M' = -\frac{1}{x^2} - \frac{1}{y} - \delta\left(\frac{1}{x} + \frac{1}{2}\right)$$

$$D_M' = -\gamma_{M,\,w}\left[\left(\frac{1}{y} - \frac{1}{x^2}\right) - \delta\left(\frac{1}{x} + \frac{1}{2}\right)\right] - \frac{\gamma_{M-1,\,w}}{x^2}$$

boundary condition 3: @ $\xi = \xi^*$, $\gamma_{u,\,w} = \gamma_f$

In order to determine the convergence and stability of

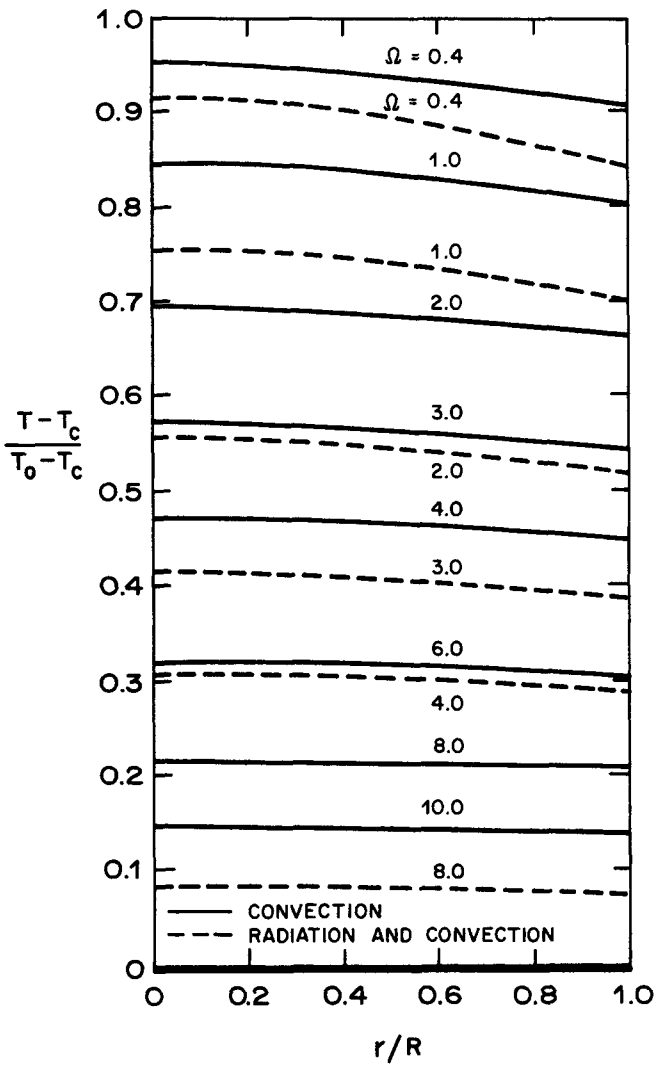

Fig. 4. Dimensionless temperature vs. radius for $hR/k_R = 0.1$, when $k_l/k_s = 1$, $\alpha_l/\alpha_s = 1$, $L/[C_{ps}(T_o-T_c)] = 0$, $T_o/T_c = 1.86$, and $\beta = 0.00371$.

the numerical method, the temperature profile of a cooling filament (neglecting the latent heat of fusion and differences in thermal diffusivity of the liquid and solid phases) was obtained using Equations (11*a*) and (14*a*). Those results were compared to the analytical solution given in Equation (15) and are plotted in Figures 3 and 4. The analytical and finite difference solutions agreed to less than 0.1% for x equal to 0.05 and y equal to 0.0025.

The method of Thomas (*4, 15*) was used to solve the numerical Equations (11*a*) and (14*a*). A marching technique was employed for evaluation of the M grid points at each w location. Through a suitable transformation of variables as suggested by Thomas, the M equations were transformed such that no matrix inversion was required and the grid points could be successively solved from the boundary condition at M to $M-1$, $M-2$, $M-3$, . . . 1.

The generalized numerical technique for solution of the cooling of a moving filament with change of state was the following. If the exit temperature of the polymer was above the freezing point, the numerical or analytical method of solution for the temperature profile in a single phase was used until the surface temperature of the filament reached the freezing point. The heat transfer problem for the two phase system was solved by considering Equations (11*a*) through (14*a*). An estimate of the distance increment (y_s) was obtained from Equation (13*a*) for

$$\xi^*_{w+1} - \xi^*_w = -x \qquad (20)$$

The initial estimate for y_s was obtained by assuming that the temperature profiles on either side of the solid-liquid interface were identical at w and $w+1$. Equation (12*a*) and boundary conditions 2 and 3 were solved by the Thomas method for the temperature profile in the solid phase. Since one desires

$$\Delta z_s = \Delta z_l \qquad (21)$$

then

$$\frac{y_s}{\alpha_s} = \frac{y_l}{\alpha_l} \qquad (22)$$

The temperature profile in the liquid phase was determined using Equations (11*a*), (22), and boundary conditions 1 and 3 with the Thomas method. Using the previously determined temperature profiles, a new estimate for the distance increment y_s could be calculated from Equation (13*a*). On the second and subsequent iterations the new value for y_s and y_l were compared to the previously obtained estimates. When the new and previous values for the distance increments were equal within a given tolerance, the temperature profile at a distance z was obtained. The solid-liquid interface was again moved as given in Equation (20) and the temperature profile calculation repeated. The method was repeated until all of the filament was solidified. Cooling of the solid strand was described by Equation (12*a*) and (14*a*) as previously discussed.

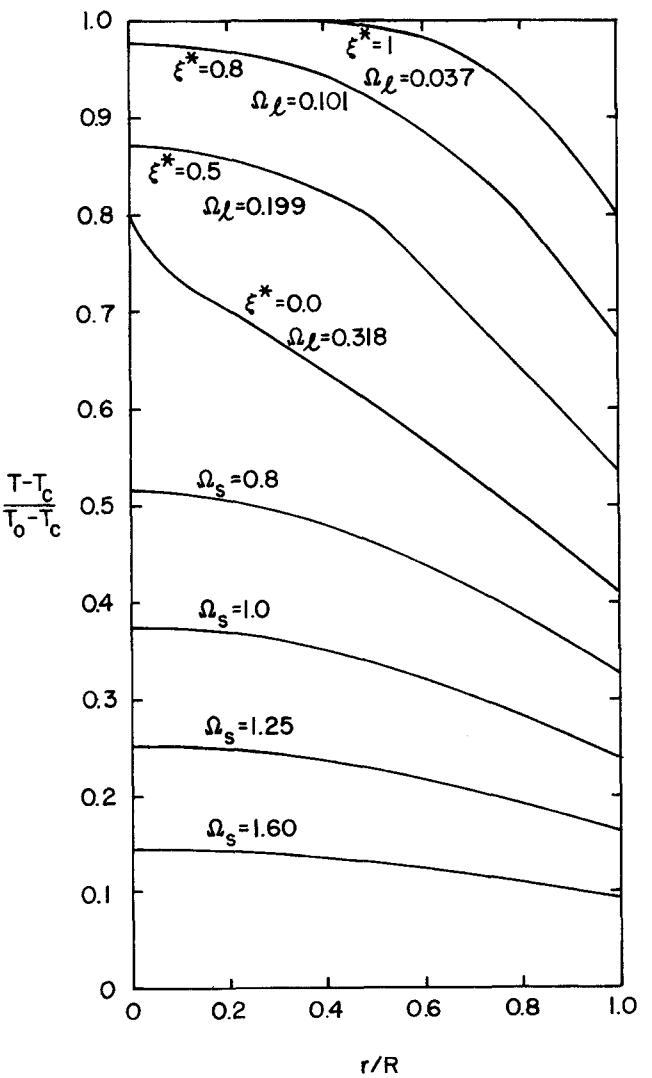

Fig. 5. Dimensionless temperature vs. radius for $hR/k_R = 1$, when $k_l/k_s = 0.5$, $\alpha_l/\alpha_s = 0.5$, $L/[C_{ps}(T_o-T_c)] = 0.25$, $\beta = 0$, and $\gamma_f = 0.8$.

The temperature profile was calculated for the case of γ_f equal to 0.8 using a high speed digital computer. The computer program is available in Fortran IV (*19*). The results are presented in Figures 5 and 6 for two different values of hR/k_R with $k_l/k_s = 0.5$, $\alpha_l/\alpha_s = 0.5$ and $L/[C_{ps}(T_0 - T_c)] = 0.25$. For the conditions stated, when the latent heat, thermal conductivity, and thermal diffusivity differences between the liquid and solid are considered, an additional distance is required to cool the filament to an equivalent temperature γ. For the cases shown in Figures 3 through 6, a 10% increase in distance Ω is required to cool the center of the filament to $\gamma = 0.1$ when the differences between the thermal properties of the liquid and solid are considered.

The effect of varying the thermal diffusivity and latent heat term ζ on the freezing of a moving filament is given in Figures 7 and 8. The effect of varying the thermal diffusivity ratio and ζ on the temperature profile is quite pronounced. A five-fold change in the thermal conductivity ratio did not affect the temperature profile. The abrupt change in slope in Figure 7 at the freezing point is due to the large difference between the thermal diffusivity of the solid and liquid phases.

Previous methods have been reported for numerical (*21*) or analog (*2*) solution of the freezing problem with the polymer initially at the freezing point. Those results were compared with calculations performed using the method

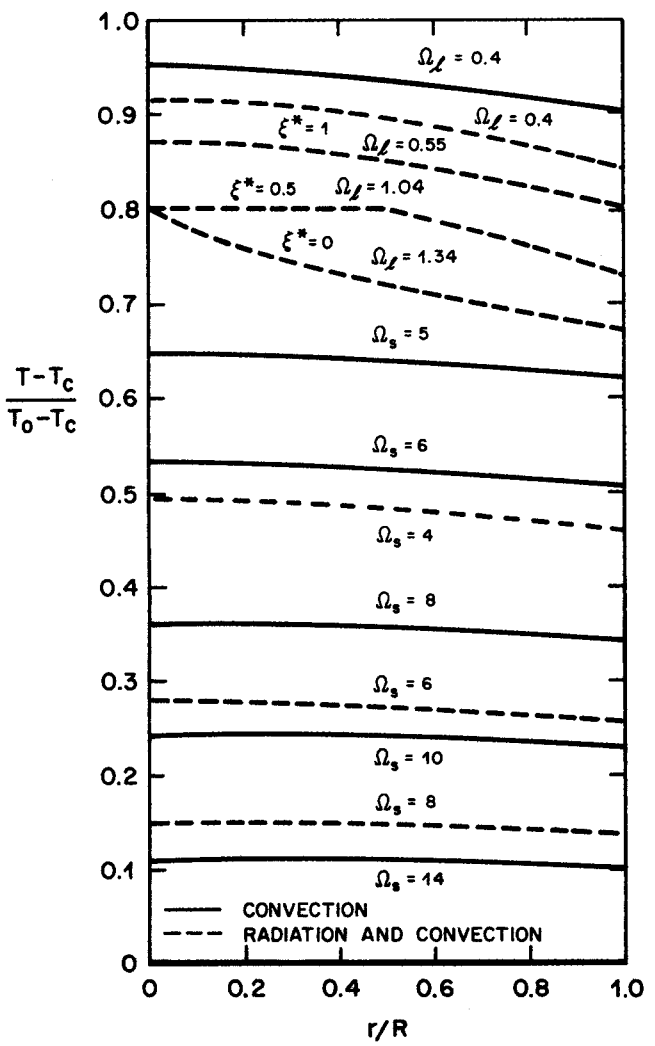

Fig. 6. Dimensionless temperature vs. radius for $hR/k_R = 0.1$, when $k_l/k_s = 0.5$, $\alpha_l/\alpha_s = 0.5$, $L/[C_{ps}(T_o-T_c)] = 0.25$, $\gamma_f = 0.8$, $T_o/T_c = 1.86$, and $\beta = 0.00371$.

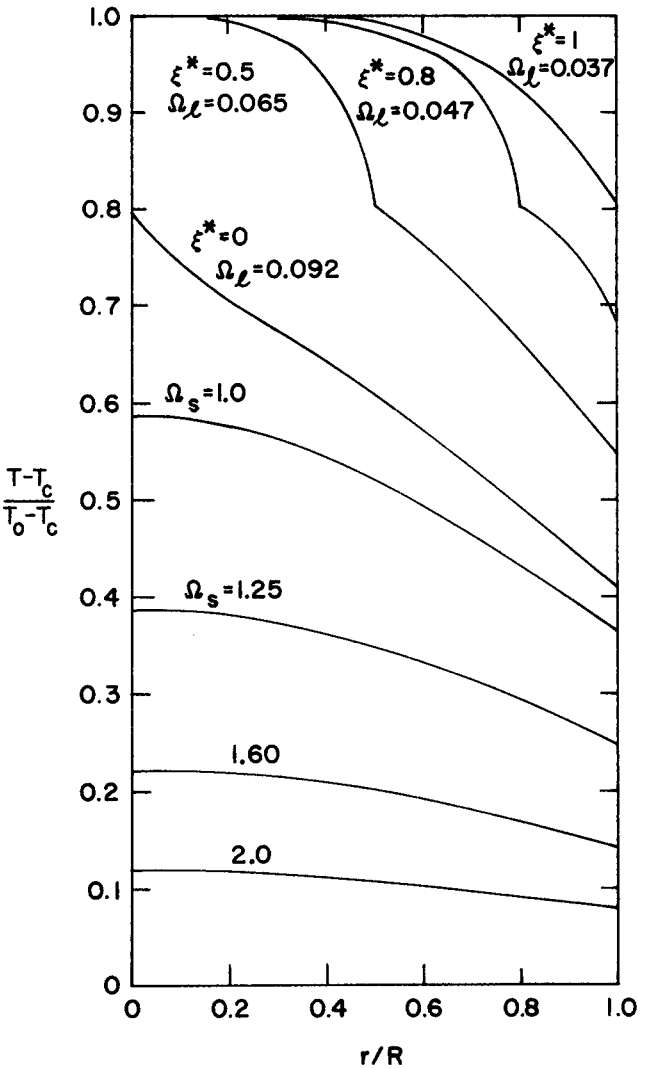

Fig. 7. Dimensionless temperature vs. radius for $hR/k_R = 1$, when $k_l/k_s = 0.5$, $\alpha_l/\alpha_s = 0.1$, $L/[C_{ps}(T_o-T_c)] = 0.25$, $\beta = 0$, and $\gamma_f = 0.8$.

described in this paper for $hR/k_R = 1.0$, $k_l/k_s = 0.5$, $\alpha_l/\alpha_s = 0.1$, $L/[C_{ps}(T_0 - T_c)] = 1.0$, and $\beta = 0$. The data presented by Tao (*21*) agree with those reported here within the accuracy of reading the plots presented in his paper. However, there is a significant difference between the data presented by Baxter (*2*) and those reported in this paper and by Tao. The data reported by Baxter do not conform to the boundary condition, Equation (6), boundary condition 2. Apparently the precision of his analog solution was not sufficient. The distance required for the solid-liquid interface to move to $\xi^* = 0.8$, 0.5, or 0 as calculated by Tao and the author do not agree with the results of Baxter. For the interface to move to $\xi^* = 0.8$, 0.5, and 0, Tao and the author report a dimensionless distance Ω_s of 0.21, 0.57, and 1.03, respectively; as compared to 0.16, 0.42, and 0.98 by Baxter.

Some question might be raised concerning the validity of assumption (7), negligible longitudinal conduction. The magnitude of the longitudinal conduction can be easily discerned by comparing the ratio of the radial and longitudinal heat flux at some point, that is

$$\frac{q_r}{q_z} = \frac{-k\dfrac{\partial T}{\partial r}}{-k\dfrac{\partial T}{\partial z}} = \frac{v_z R}{\alpha_s}\,\frac{\dfrac{\partial \gamma}{\partial \xi}}{\dfrac{\partial \gamma}{\partial \Omega_s}} \qquad (23)$$

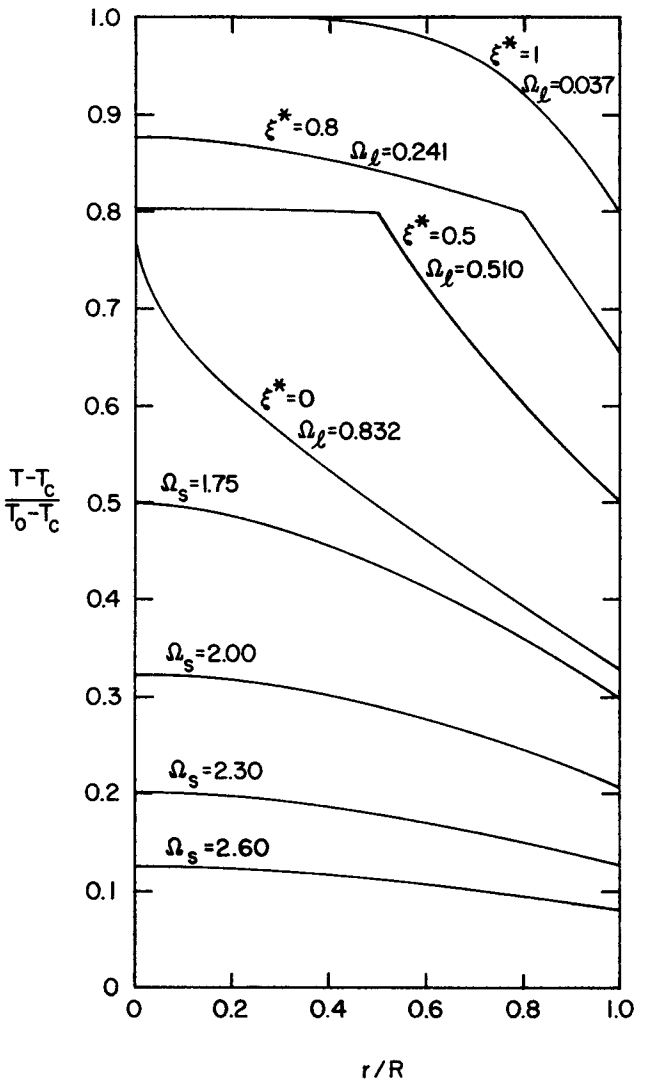

Fig. 8. Dimensionless temperature vs. radius for $hR/k_R = 1$, when $k_l/k_s = 0.5$, $\alpha_l/\alpha_s = 0.5$, $L/[C_{ps}(T_o-T_c)] = 1.25$, $\beta = 0$, and $\gamma_f = 0.8$.

For melt spinning of most textile fibers, v_zR/α_s is of the order of 10^5. Therefore longitudinal conduction is only important when the ratio

$$\frac{\dfrac{\partial\gamma}{\partial\xi}}{\dfrac{\partial\gamma}{\partial\Omega_s}} \lesssim 10^{-4} \qquad (24)$$

By examination of Figures 3 through 8, the validity of assumption (7) can be readily established.

One must always discern the relative importance of radiative and convective energy transport in any physical system, especially when the Nusselt number is small or the surface temperature is high. Heat transfer from the filament to the surroundings by simultaneous convective and radiative energy transport can be described by the above method, with the exception of Equation (6), boundary condition 2. The boundary condition must be changed to:

$$\text{boundary condition 2:} \quad @\ r = R, \quad -k_R \left.\frac{\partial T}{\partial r}\right|_R = h(T_R - T_c) + \sigma\epsilon_p T_R^4 - \sigma\epsilon_w a_p T_w^4 \qquad (25)$$

If we assume that $\sigma\epsilon_p T_R^4 >> \sigma a_p \epsilon_w T_w^4$ and insert the dimensionless variables, Equation (25) reduces to:

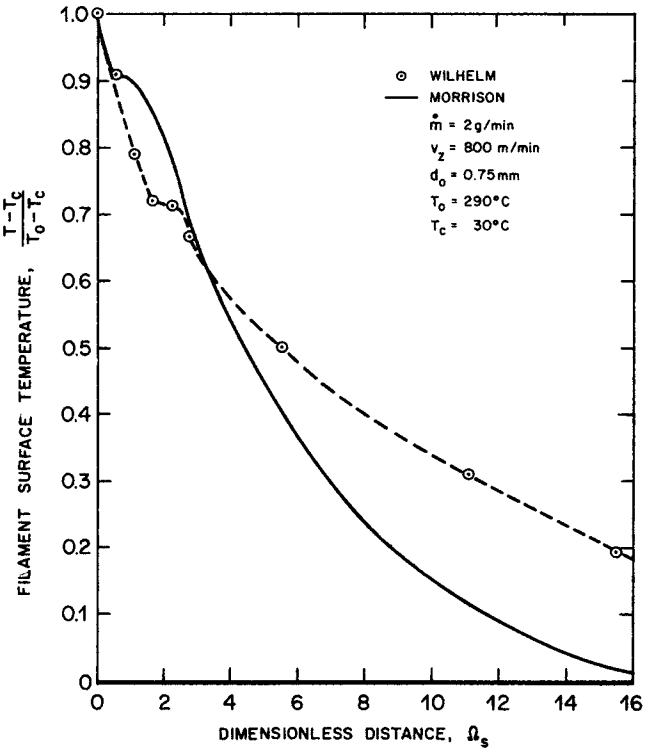

Fig. 9. Comparison between theory and experiment. Dimensionless temperature vs. radius for $hR/k_R = 0.05$, when $k_l/k_s = 0.5$, $\alpha_l/\alpha_s = 0.472$, $L/[C_{ps}(T_o-T_c)] = 0.165$, $\gamma_f = 0.904$, $\beta = 0.00371$, and $T_o/T_c = 1.86$.

$$\text{boundary condition 2:} \quad @\ \xi = 1, \quad -\left.\frac{\partial\gamma}{\partial\xi}\right|_R = \frac{hR}{k_R}\gamma_R + \frac{\sigma\epsilon_p R(T_0 - T_c)^3}{k_R}\left[1 + \gamma_R\left(\frac{T_0}{T_c} - 1\right)\right]^4 \gamma_R^4 \qquad (26)$$

The numerical method was used to discern the relative importance of radiative and convective energy transport in the system described above. Figures 4 and 6 show for $hR/k_R = 0.1$, that radiative energy transport must be considered. The values of the dimensionless variables are representative for the spinning of polyamides, polyesters, polypropylene, and other melt spun fibers. For these systems, one can essentially neglect radiative energy losses when $hR/k_R \gtrsim 0.5$

Before discussing the agreement between theory and experiment some consideration should be given to the validity of the mathematical model. The film heat transfer coefficient (h) in Equation (6) and (25) was assumed to be invariant with position. A coolant flow perpendicular to the filament traverse is used in practice. That may produce a heat transfer coefficient which is angularly dependent. One would suspect only a small variation with angle, since the coolant velocity is usually quite small. The radius of the filament will vary with distance (z). That may cause a significant variation in the film heat transfer coefficient. Using the data reported by Wilhelm (23) one sees that the decrease in filament radius creates no important radial velocity component. The emissivity and absorptivity have been assumed constant. They may vary in actual practice. The inert gaseous coolant was assumed to be transparent to radiative energy transport. Since the coolant is generally maintained at approximately the same temperature as the surrounding walls and in most cases is a diatomic homonuclear molecule, the assumption seems warranted.

It would be of considerable interest to compare the theoretical results presented in this paper with experimental data. Very limited experimental data are available for the variance of surface temperature with distance from the spinneret. Wilhelm (*23*) has reported experimental surface temperature and filament diameter as a function of distance from the spinneret for a polyester; while Kase and Matsuo (*12*) report similar data for polypropylene. Thermodynamic data for polyethylene terephthalate is available in the literature (*9, 10, 13, 14*). However, there is a large disagreement between various authors for the value of these properties. Using representative values for the thermodynamic properties and a Nusselt number of 0.562, the theory described in this paper was used to predict filament surface temperature as a function of distance from the spinneret. The results are compared with the data reported by Wilhelm in Figure 9. The shape of both curves are very similar. One clearly sees that the polyester studied by Wilhelm did not have a clearly defined melting point at $\gamma = 0.904$, which is reported by Ke (*13*) for polyethylene terephthalate. The heat transfer coefficient is also seen to be a function of distance from the spinneret. Experimental data for surface temperature and filament diameter as a function of distance from the spinneret for a well characterized polymer is very urgently needed. A value for the heat transfer coefficient could be easily obtained if that information were available. Using the above described technique with accurate thermodynamic and heat transfer coefficients, quenching apparatus for melt spun fibers could be easily designed. Too often in the past, that equipment has been designed by costly trial-and-error methods.

CONCLUSION

A general technique can be described for the numerical solution of the equations which depict solidification in the cylindrical coordinate system. The method can be applied to the cooling and solidification of a moving filament of polymer. Considering both convective and radiative energy losses, the solution is given in terms of six dimensionless variables: α_l/α_s, k_l/k_s, hR/k_R, $L/[C_{ps}(T_0 - T_c)]$, T_0/T_c, and $\sigma\epsilon_p R(T_0 - T_c)^3/k_R$. The thermal properties which affect the temperature profiles and freezing times most markedly are α_l/α_s, $L/[C_{ps}(T_0 - T_c)]$, hR/k_R and β. Radiative energy losses must be considered when hR/k_R is less than approximately 0.5 for most molten polymers. The form of the theoretical equation compares very favorably with experimental data. However, the dearth of thermodynamic data in conjunction with temperature measurements precludes a better fit between theory and experiment at this time. Experimental thermodynamic and surface temperature data are urgently required such that accurate values for the heat transfer coefficient can be calculated.

NOTATION

a = absorptivity, dimensionless
C_p = heat capacity at constant pressure, cal./g.°K.
d_0 = diameter of spinneret holes, mm.
D = filament diameter, cm.
h = film heat transfer coefficient, cal./sq.cm. sec. °K.
J_n = Bessel function of order n
k = thermal conductivity, cal./cm. °K. sec.
L = latent heat of fusion, cal./g.
M = number of grid points in ξ direction
N_{Nu} = Nusselt number, hD/k_c
P = pressure, dynes/sq.cm.
R = filament radius, cm.
t = time, sec.
T = temperature, °K.
u = grid points in ξ direction for numerical solution
V = specific volume, cc./g.
v = velocity, cm./sec.
w = grid points in Ω direction for numerical solution
x = grid spacing in ξ direction for numerical solution
y = grid spacing in Ω direction for numerical solution
r, θ, z = cylindrical coordinates

Greek Letters

α = thermal diffusivity, sq.cm./sec.
β = dimensionless radiation group, $\sigma\epsilon_p R(T_0 - T_c)^3/k_R$
δ = dimensionless group, hR/k_R
ϵ = emissivity, dimensionless
ζ = dimensionless group, $L/[C_{ps}(T_0 - T_c)]$
ξ = dimensionless radius, r/R
ρ = density, g./cc.
σ = Stefan-Boltzmann constant, 0.1712×10^{-8} B.t.u./hr. sq.ft. R^4
γ = dimensionless temperature, $(T - T_c)/(T_0 - T_c)$
γ_v = shear stress, dynes/sq.cm.
Ω = dimensionless distance, $z\alpha/v_z R^2$

Subscripts

c = inert gaseous coolant
f = freezing
l = liquid
0 = at distance $z = 0$
p = polymer
R = filament wall
s = solid
w = surrounding walls
r, θ, z = coordinate directions
* = solid-liquid interface

LITERATURE CITED

1. Allen, D. N. De. G., and R. T. Severn, *Quart. J. Mech. Appl. Math.*, **5**, 447 (1952).
2. Baxter, D. C., *J. Heat Transfer*, **84**, 317 (1962).
3. Bird, R. B., W. E. Stewart, E. N. Lightfoot, "Transport Phenomena," p. 322, John Wiley, New York (1960).
4. Bruce, G. H., D. W. Peaceman, H. H. Rachford, and J. D. Rice, *Trans. Am. Inst. Mech. Engrs.*, **198**, 79 (1953).
5. Carslaw, H. S., and J. C. Jaeger, "Conduction of Heat in Solids," p. 282, Oxford University Press, London, England (1959).
6. Ibid., p. 202.
7. Crank, J., *Quart. J. Mech. Appl. Math.*, **10**, 220 (1957).
8. Danckwerts, P. V., *Trans. Faraday Soc.*, **46**, 701 (1950).
9. Dole, M., *J. Polymer Sci.*, **20**, 37 (1956).
10. Eiermann, K., and K. H. Hellwege, *ibid.*, **57**, 99 (1962).
11. Hrycak, P., *AIChE J.*, **13**, 160 (1967).
12. Kase, S., and T. Matsuo, *J. Applied Polymer Sci.*, **11**, 257 (1967).
13. Ke, B., *ibid.*, **6**, 624 (1962).
14. Keller, A., G. R. Lester, and L. B. Morgan, *Royal Soc. London Phil. Trans.*, **247**, A921, 1 (1954).
15. Lapidus, L., "Digital Computation for Chemical Engineers," p. 254, McGraw-Hill, New York (1962).
16. Lin, S., *V. D. I. Zeitschrift*, **106**, 1379 (1964).
17. London, A. L., and R. A. Seban, *Trans. Am. Soc. Mech. Engrs.*, **65**, 771 (1943).
18. Longwell, P. A., *AIChE J.*, **4**, 53 (1958).
19. Morrison, M. E., *ARL 68-0064*, ARL (ARC), Wright-Patterson Air Force Base, Ohio (1968).
20. O'Brien, G. G., M. A. Hyman, and S. Kaplan, *J. Math. Phys.*, **29**, 223 (1951).
21. Tao, L. C., *AIChE J.*, **13**, 165 (1967).
22. Wilcox, W. R., and D. L. Duty, *J. Heat Transfer*, **88C**, 45 (1966).
23. Wilhelm, G., *Kolloid-Zeitschrift Zeitshrift für Polymere*, **208**, 97 (1966).

Manuscript received March 21, 1968; revision received May 31, 1968; paper accepted June 28, 1968.